The effect of boron on the electronic structure of grain boundaries in Ni_3Al

1996 J. Phys.: Condens. Matter 8 5527

(http://iopscience.iop.org/0953-8984/8/30/004)

J. Phys.: Condens. Matter **8** (1996) 5527–5534. Printed in the UK

The effect of boron on the electronic structure of grain boundaries in Ni_3Al

Wang Fuhe†, Wang Chongyu†‡ and Yang Jinlong§

† Central Iron and Steel Research Institute, Beijing 100081, People's Republic of China
‡ China Centre of Advanced Science and Technology (World Laboratory), Beijing 100080, People's Republic of China
§ Centre for Fundamental Physics, University of Science and Technology of China, Hefei, Anhui 230026, People's Republic of China

Received 20 February 1996, in final form 16 April 1996

Abstract. The electronic structure of $\Sigma 5[001](210)$ and $\Sigma 13[001](320)$ grain boundaries in Ni_3Al containing B are investigated by the use of the discrete variational method. The effects of B on Ni_3Al grain boundaries are discussed. The results show that B forms stronger bonding states with its neighbouring host atoms, and it can be expected that the cohesive strength of the grain boundaries will be increased.

1. Introduction

Grain boundaries are important defects in materials; they are closely tied in with the properties of alloys. Studies of the effects of impurities (such as B, C, S, P and H) on the embrittlement of metal and intermetallic compounds provide the foundation for increasing the strength levels of materials. There have been some experimental and theoretical studies in this field; the polyhedral cluster model has been used to represent the local environment of grain boundaries doped with impurities and to study the electronic structure of materials containing structural defects [1–5]. Messmer and Briant [1, 2] reported the effect of the doping in the grain boundaries on the features of bonding. Their results showed that if boron is in the interstices of a nickel grain boundary, in addition to the charge in the metal bonds across the grain boundary not decreasing, a covalent-like bond is formed between the boron and the host metal. This bonding will give additional cohesiveness across the grain boundary. Hashimoto *et al* [6] and Wang and Zhao [7], using the recursion method, studied the action of the B and P in grain boundaries of Fe, and B, N and P in grain boundaries of Ni respectively; the results are similar to Messmer's. Goodwin *et al* [8] and Needels *et al* [9], using the pseudopotential total energy technique, calculated the interlayer cohesive energy of Al and the total energy of grain boundaries for Au. With the rapid development of computer technology, one can study the electronic structure of grain boundaries in a larger cluster or embedded cluster from first principles. Recently, Tang, Freeman and Olson used the DMol method [10] to study the electronic structure of B and S/Fe $\Sigma 3$ grain boundaries, and provided useful information revealing the nature of the embrittlement for the Fe $\Sigma 3$ grain boundary.

Ni_3Al with the $L1_2$ structure is ductile as a single crystal, but it is intergranularly brittle in the polycrystalline state [11]. It is found that the brittleness of grain boundaries in Ni_3Al

0953-8984/96/305527+08$19.50

is intrinsic [11]. However, when the intermetallic compound Ni_3Al is doped with a small amount of boron the tendency towards intergranular fracture is reduced significantly [12]. Two mechanisms were proposed to explain how the segregation of boron at grain boundaries improves the ductility. One of these is that B segregated at grain boundaries will increase the cohesive strength of the grain boundaries by the formation of strong metallic bonds [13, 14]. The other is that B segregated at grain boundaries reduces atomic ordering in the grain boundary regions and this results in the increase of the mobility of dislocations in grain boundaries [15, 16], or of the number of available dislocation reactions at the grain boundaries [17], or both [18]. Whether or not this mechanism successfully explains the effect of B on Ni_3Al grain boundaries has not been decided as yet.

Chaki proposed a model for explaining the effect of boron on the ductility of Ni-rich Ni_3Al [19, 20]. It is argued that the interstitial boron and antisite Ni atoms distort bonds and reduce the directionality or the strength of Ni–Al bonds in the interior of the grains in Ni_3Al. This makes generation and propagation of dislocations easier in the grains. Chen *et al*, using atomistic simulations, studied the structure of Ni_3Al grain boundaries [21] and the effects of boron on Ni_3Al grain boundaries [22]. Their results showed that boron is found to segregate more strongly to grain boundaries than to free surfaces, and the boron segregation at grain boundaries will increase the grain boundary cohesive strength. In addition, Eberhart and Vvedensky calculated the density of states of Ni_3Al grain boundaries using a multiple-scattering (MS) X_α method with a small cluster [5]. Their calculated result showed that the appearance of localized grain boundary states near the Fermi level is an indicator that a compound is prone to intergranular fracture, and indicated that the mechanical stability of the grain boundary is decreased compared to that of the parent crystal of Ni_3Al.

In this paper, the discrete variational (DV) method [23–26] within the framework of density functional theory is used to study the effect of boron on Ni_3Al grain boundaries. The methodology and the model are presented in section 2, the calculated results are discussed in section 3, and we give some conclusions in the last section.

2. The computation method and cluster model

The discrete variational method (DVM) which is a first-principles numerical method for solving the local density functional equations [23–26] is used to study the electronic structure of grain boundaries in Ni_3Al and the effect of boron. In this paper, the embedded-cluster approach is used, and the charge density of several hundreds of atoms surrounding the grain boundary is considered in constructing the self-consistent potential.

In the one-electron-like wave equation, the Hamiltonian is

$$H = -\nabla^2/2 + V_c + V_{xc} \tag{1}$$

where V_c is the electron–nucleus and electron–electron Coulomb potential, and V_{xc} derived by Von Barth and Hedin [27] is the exchange–correlation potential. The eigenstates (or molecular orbitals) are expanded as linear combinations of atomic orbitals $\phi_i(r)$ [26]:

$$\psi_n(r) = \sum_i C_{ni}\phi_i(r). \tag{2}$$

In order to study the interaction between atoms, the interatomic energy between atom l and atom m is derived [7, 28]:

$$E_{lm} = \sum_n \sum_{\alpha\beta} N_n a^{\star}_{n\alpha l} a_{n\beta m} H_{\beta m\alpha l} \tag{3}$$

where N_n is the occupation number for molecular orbital ψ_n, $a_{n\alpha l} = \langle \phi_{\alpha l}(r)|\psi_n(r)\rangle$, and $H_{\beta m\alpha l}$ is the Hamiltonian matrix element connecting the atomic orbital β of atom m and the atomic orbital α of atom l.

In the computation, the single-site orbitals are used as the basis set, and the frozen-core mode is chosen; also the funnel potential is introduced. The non-spin-polarized secular equations are solved using the self-consistent-charge (SCC) approximation.

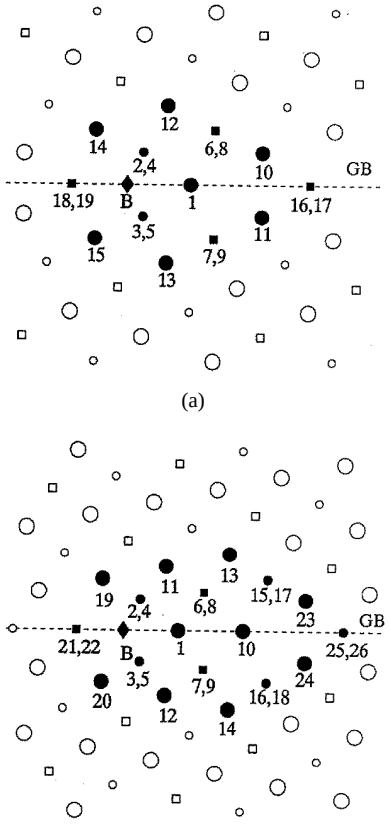

Figure 1. The atomic configurations around tilt grain boundaries in Ni_3Al. The Ni and Al atoms are represented by the circles and squares; the different sizes represent different layers. The atoms shown as solid symbols and labelled by numbers are in the cluster; the solid diamonds represent the B atom. (a) $\Sigma 5[001](210)$; (b) $\Sigma 13[001](320)$.

The grain boundaries $\Sigma 5[001](210)$ and $\Sigma 13[001](320)$, which are constructed by use of the coincidence site lattice model [29, 30] and atomistic simulations [21], are investigated. Figures 1(a) and 1(b) show the atomic configurations for $\Sigma 5$ and $\Sigma 13$ grain boundaries. The cluster atoms shown as solid symbols (in figure 1) are embedded in several hundreds of surrounding atoms. In order to discuss the interaction between atoms clearly, the atoms in the cluster are labelled with numbers. With a method like that of Masuda-Jindo [31], the atomic relaxation is carried out by the energy-minimization procedure in which a proportion of the atoms at grain boundaries are pulled apart from the interface. When the minimum of the binding energy is achieved for the cluster system, the equilibrium configuration is given.

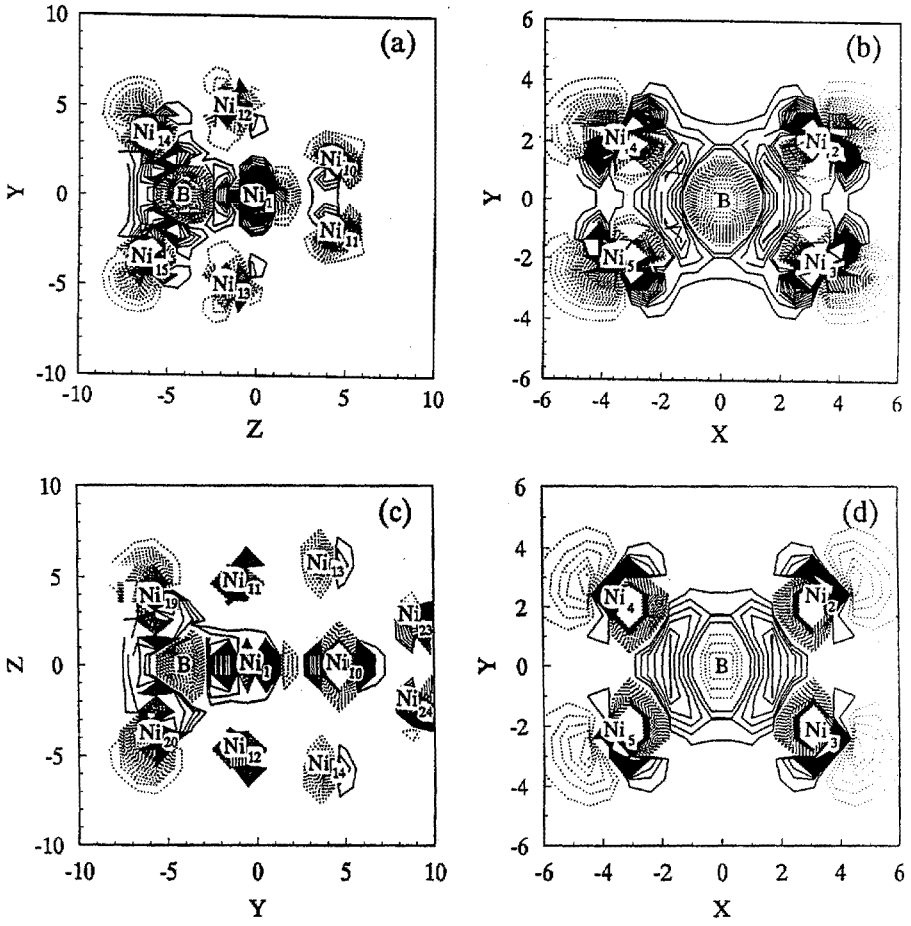

Figure 2. The charge-density difference between the B-doped grain boundary and a superposition of a single B atom and clean grain boundary, (a) and (b) for Σ5[001](210), and (c) and (d) for Σ13[001](320) tilt grain boundaries in Ni_3Al. The contour spacings are $0.001e$ au^{-3}. Solid lines indicate a gain of charge and dashed lines indicate a loss of charge.

3. Results and discussion

3.1. Charge density

The charge-density difference is obtained by subtracting the charge density of the clean grain boundary and a free boron atom from the charge density of the B-doped grain boundary. So that the boron-induced charge redistribution can be seen more clearly [10], we show in figure 2 the charge-density difference plotted in the Y–Z plane which contains nickel atoms and boron, and the X–Y plane which contains Ni_2, Ni_3, Ni_4 and Ni_5 atoms and is near to the boron.

In figure 2, it can be seen that the charge density in the intermediate region between boron and its near-neighbour atoms is obviously increased, but the charge density between Ni_2 and Ni_3 (or Ni_4 and Ni_5) host atoms (these pairs of atoms are across the grain boundaries) is hardly affected by the boron. This is similar to the behaviour of boron in the B-doped nickel grain boundaries [1, 2]. The results for Σ5 and Σ13 grain boundaries indicate

that boron forms relatively strong bonds with its neighbouring atoms. Thus this can be regarded as the B atom acting as a 'bridge' and increasing the cohesive strength of the grain boundaries. The above calculated results are in agreement with the atomistic simulation study [22]. Meanwhile, from the calculation of the charge-density difference it can also be found that the effect of boron on the host atoms is localized in the region near to the boron. The feature is also found in the B/Fe $\Sigma 3$ grain boundary system [10].

Table 1. The interatomic energies (in eV) of the adjacent atoms in grain boundaries with (E_{GB+B}) and without (E_{GB}) B atoms; $\Delta E = E_{GB+B} - E_{GB}$ is the change of interatomic energy induced by the addition of a B atom.

Pairs of atoms	$\Sigma 5$			$\Sigma 13$		
	E_{GB}	E_{GB+B}	ΔE	E_{GB}	E_{GB+B}	ΔE
Ni_1–Ni_2	−1.399	−1.176	0.223	−1.447	−1.223	0.224
Ni_2–Ni_3	−4.048	−3.649	0.399	−3.091	−2.932	0.159
Ni_1–Al_6	−1.263	−1.279	−0.016	−1.441	−1.488	−0.047
Ni_1–Ni_{12}	−1.232	−1.222	−0.010	−1.479	−1.534	−0.055

Table 2. The interatomic energies E_{B-l} (in eV) between the B atom and its adjacent atoms.

	$\Sigma 5$				$\Sigma 13$			
	B–Ni_1	B–Ni_2	B–Ni_{14}	B–Al_{18}	B–Ni_1	B–Ni_2	B–Ni_{19}	B–Al_{21}
E_{B-l}	−2.477	−2.326	−2.892	−0.747	−2.608	−2.009	−2.962	−1.044

3.2. Interatomic energy

The interatomic energies defined by equation (3) are calculated, and the results are listed in tables 1 and 2. From table 1, we can find that the energy of interaction between host atoms which are close to B atoms, such as the pairs of Ni_1–Ni_2 and Ni_2–Ni_3, is weakened by the addition of B atoms. However, the energy of interaction between host atoms which are not near B atoms, such as Ni_1–Al_6 and Ni_1–Ni_{12} pairs, is slightly changed by the addition of B.

From table 2, it can be seen that the energy of interaction between boron and its neighbouring atoms is very strong; this is closely related to the cohesion of the grain boundary, and is consistent with the calculated results for the charge density. On the basis of the calculation of the interatomic energy, it can be predicted that the B atom will enhance the grain boundary and thus inhibit intergranular fracture. The theoretical results from first-principles numerical calculations are in agreement with the experimental results [13] and the atomistic simulation study [22]. In addition, our calculated results also show that the bonding formed by boron with nickel is very strong, and that the interaction between Ni and Al ($E_{Ni_1-Al_6}$) is not decreased by the addition of B atoms. This is at variance with Chaki's suggestion that the interstitial B atoms in Ni-rich Ni_3Al reduce the strength of the directional bonding between Ni and Al atoms in the interior of the grains [20].

In order to discuss the influence of the deviation from stoichiometric composition on the ductility of B-doped Ni_3Al alloy, the interatomic energies of several other clusters belonging

to the Σ5 and Σ13 grain boundaries are calculated. One typical cluster is shown in figure 4, in which the centre of the cluster is translated from the Ni_1 atom to the Al_{16} atom associated with figure 1(a). The typical interatomic energies for the boron and Ni atoms from the Σ5 grain boundary shown in figure 1(a) are assigned as $E_{B-Ni_1} = -2.477$ eV and $E_{B-Ni_{14}} = -2.892$ eV, and the corresponding interatomic energies in the other Σ5 cluster shown in figure 4 are $E'_{B-Al_1} = -2.124$ eV and $E'_{B-Al_{14}} = -2.413$ eV respectively. The results indicate that the interaction between B and Ni is stronger than that between B and Al, and so the B atom tends to interact with Ni atoms rather than with Al atoms. Therefore it can be predicted that the amount of boron segregated to the grain boundary will be decreased with the increase of aluminium concentration in Ni_3Al, and that the effect of boron on the ductility of Ni_3Al will become less when the content of boron is less than the critical amount at the grain boundary [13].

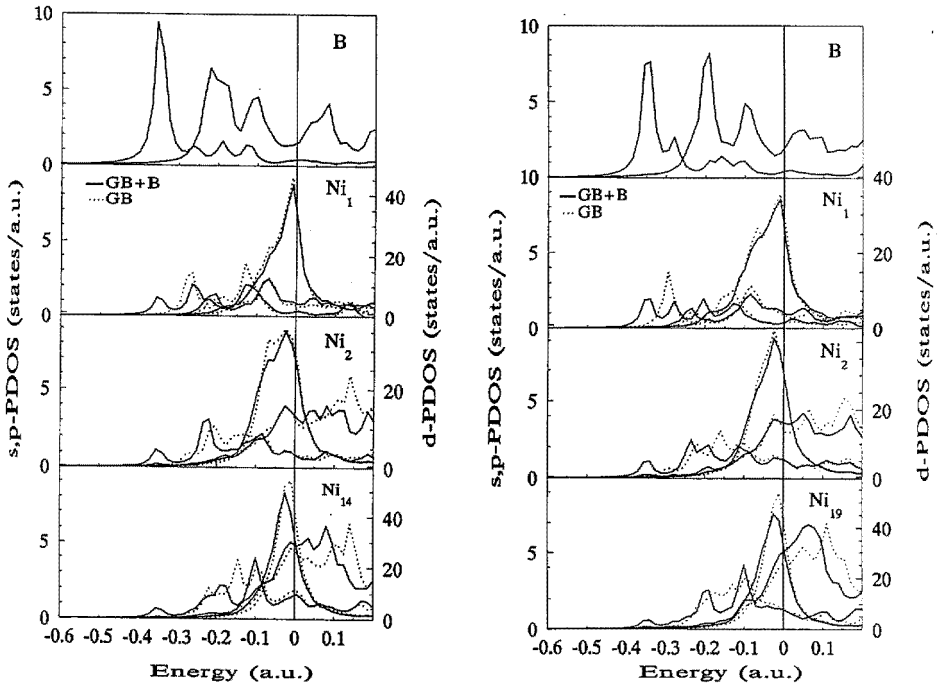

Figure 3. The partial densities of states (PDOS) of a B atom and its neighbouring atoms for (a) Σ5(210) and (b) Σ13(320) tilt grain boundaries in Ni_3Al. The solid and broken lines represent the PDOS of doped and clean grain boundaries respectively.

4. Density of states

The densities of states (DOS) are obtained by broadening the discrete eigenvalue spectrum with a set of Lorentz functions. The partial densities of states (PDOS) of a B atom and its neighbouring Ni atoms are shown in figure 3. Comparing the DOS of a B-doped grain boundary with that of a clean grain boundary, some features can be noted. First, the s and d PDOS of the host atoms are moved towards deep potential wells with the addition of B. Second, a hybridization between B sp and Ni sd takes place. However, the p PDOS of host

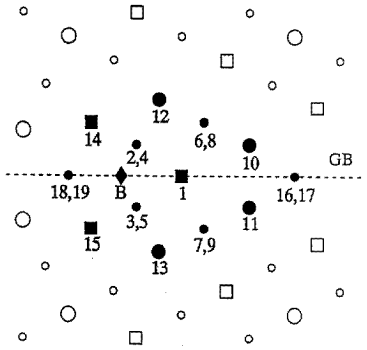

Figure 4. The calculated atomic configuration of another cluster which belongs in the $\Sigma 5[001](210)$ tilt grain boundary in Ni_3Al. The meaning of the symbols is the same as in figure 1.

atoms are hardly affected by the addition of B. From the point of view of energetics, this can be regarded as B making the grain boundary more stable and enhancing the cohesion of the grain boundary. In addition, it can be found that the changes of the DOS near the Fermi level induced by the addition of B arise mainly from changes of the d PDOS, while the s and p PDOS are almost unchanged. The reduction of the DOS near the Fermi level means that the transition probability of electronic states is confined; thus the addition of B may be beneficial to the stability of grain boundaries. This is consistent with the (MS) X_α calculation [5].

Table 3. The electron occupation number n in valence orbitals and the changes ($\Delta n = n(\mathrm{GB}+\mathrm{B}) - n(\mathrm{GB})$) induced by the addition of a B atom.

		Ni_1			Ni_2			Ni_{14} (Ni_{19})		
		3d	4s	4p	3d	4s	4p	3d	4s	4p
$\Sigma 5$	n(GB)	8.368	0.738	0.542	8.227	0.959	0.857	8.211	1.098	0.767
	n(GB+B)	8.396	0.728	0.597	8.240	0.934	0.931	8.226	1.037	0.870
	Δn	0.028	−0.010	0.055	0.013	−0.025	0.074	0.015	−0.061	0.103
$\Sigma 13$	n(GB)	8.372	0.764	0.609	8.251	1.041	0.762	8.246	1.171	0.589
	n(GB+B)	8.388	0.742	0.711	8.266	0.990	0.838	8.251	1.105	0.730
	Δn	0.016	−0.022	0.102	0.015	−0.051	0.076	0.005	−0.066	0.141

The electron occupation number of orbits is calculated by use of Mulliken analysis; the results are presented in table 3. From the calculated results, it can be seen that the number of electrons in 4s orbitals of host Ni atoms decreases with the addition of B, while the numbers of electrons in 3d and 4p orbitals increase. The weakening of the directional bonding states formed by p and d orbitals may be related to the characteristic of fracture of the grain boundary and reflects the boron being a cohesion enhancer.

5. Conclusion

We have performed a first-principles numerical calculation to study the effect of B on the grain boundaries in Ni_3Al. It is found that a strong bonding between B and the host atoms is formed, and that the B–Ni bonding strength is larger than that for B–Al. This suggests that the B will 'prefer' to segregate at Ni-rich grain boundaries, rather than stoichiometric or Al-rich boundaries. On the other hand, the addition of boron results in the DOS shifting

towards the deep energy region and reduces the DOS near the Fermi level; this is a mark of the stability of the system. It can be concluded that as a cohesion enhancer, B segregated at grain boundaries will improve the ductility of polycrystalline Ni_3Al in Ni-rich cases.

Acknowledgment

This work was supported by the National Natural Science Foundation of China.

References

[1] Briant C L and Messmer R P 1980 *Phil. Mag.* B **42** 569
[2] Messmer R P and Briant C L 1982 *Acta Metall.* **30** 457
[3] Painter G S and Averill F W 1987 *Phys. Rev. Lett.* **58** 234
[4] Eberhart M E, Latanision R M and Johnson K H 1985 *Acta Metall.* **33** 1769
[5] Eberhart M E and Vvedensky D D 1987 *Phys. Rev. Lett.* **58** 61
[6] Hashimoto M, Ishida Y, Wakayama S, Yamamoto R, Doyama M and Fujiwara T 1984 *Acta Metall.* **32** 13
[7] Wang C Y and Zhao D L 1994 *Mater. Res. Soc. Symp. Proc.* **318** 571
[8] Goodwin L, Needs R J and Heine V 1988 *Phys. Rev. Lett.* **60** 2050
[9] Needels M, Rappe A M, Bristowe P D and Joannopoulos J D 1992 *Phys. Rev.* **46** 9768
[10] Tang S, Freeman A J and Olson G B 1994 *Phys. Rev.* B **50** 1
[11] Liu C T 1991 *Scr. Metall.* **25** 1231
[12] Aoki K and Izumi O 1979 *J. Japan Inst. Met.* **43** 1190
[13] Liu C T, White C L and Horton J A 1985 *Acta Metall.* **33** 213
[14] White C L, Padgett P A, Liu C T and Yalisov S M 1985 *Scr. Metall.* **18** 1417
[15] Schulson E M, Weihs T P, Baker I, Frost H J and Horton J A 1986 *Acta Metall.* **34** 1395
[16] Weihs T P, Zinoviev V, Viens D V and Shulson E M 1987 *Acta Metall.* **35** 1104
[17] King A H and Yoo M Y 1987 *Mater. Res. Soc. Symp. Proc.* **81** 99
[18] George E P, White C L and Horton J A 1991 *Scr. Metall.* **25** 1259
[19] Chaki T K 1990 *Phil. Mag. Lett.* **61** 5
[20] Chaki T K 1991 *Phil. Mag. Lett.* **63** 123
[21] Chen S P, Voter A F and Srolovitz D J 1986 *Scr. Metall.* **20** 1389
[22] Chen S P, Voter A F, Albers R C, Boring A M and Hay P J 1990 *J. Mater. Res.* **5** 955
[23] Ellis D E and Painter G S 1970 *Phys. Rev.* B **2** 2887
[24] Ellis D E, Benesh G A and Bykom E 1977 *Phys. Rev.* B **16** 3308
[25] Delley B, Ellis D E and Freeman A J 1983 *Phys. Rev.* B **27** 2132
[26] Guenzburger D and Ellis D E 1992 *Phys. Rev.* B **46** 285
[27] Von Barth U and Hedin L 1972 *J. Phys. C: Solid State Phys.* **5** 1629
[28] Wang C Y, Du C Y, Zeng Y P, Gao L and Liu F S 1989 *Proc. Int. Workshop on Physics of Materials (Shenyang)* B5-1
[29] Izumi O and Takasugi T 1988 *J. Mater. Res.* **3** 426
[30] Takasugi T and Izumi O 1983 *Acta Metall.* **31** 1187
[31] Masuda-Jindo K 1982 *J. Physique* **43** 921